Postbuckling Behavior of Anisotropic Laminated Plates Under Pure Shear and Shear Combined with Compressive Loading

Y. Zhang* and F. L. Matthews†
Imperial College of Science and Technology, London, United Kingdom

In the current work a postbuckling analysis for anisotropic plates under combined compressive and shear loading is presented. A pair of governing equations in the von Kármán sense are solved in conjunction with simply supported boundaries. A series of computations is carried out for plates having different lay-ups, different materials, and different aspect ratios. The emphasis of these investigations is put on the effect of shear direction on the postbuckling behavior of the plates. The results of the computations reveal that the postbuckling behavior of anisotropic plates is completely different when the applied shear directions are alternated for the plate under either shear loading or combined loading.

Introduction

THE postbucking behavior of composite plates under shear loading has been studied experimentally by a few investigators.[1-3] It was reported that the ultimate loads of plates made of boron/epoxy, carbon/epoxy, or graphite /epoxy could be considerably higher than the initial buckling loads. However, so far, few postbuckling analyses are available for anisotropic plates under shear or combined loading.

In previous work[4-6] it was pointed out that the shear direction has a significant influence on the initial buckling behavior of anisotropic plates under pure shear or under the combination of compressive and shear loading. Thus it is natural to raise the question: How does the shear direction affect the postbuckling behavior of the anisotropic plates? The present work answers the question.

In the current work a postbuckling analysis for plates of composite material with midplane symmetric lay-up is presented. A pair of governing equations in the von Kármán sense, in which the effects of boundary moments are included, are solved in conjunction with simply-supported boundaries. As examples, a series of computations are carried out for plates having different fiber directions, different stacking sequences of layers, different materials, and different aspect ratios. The results reveal that the direction of applied shear with respect to the fibers of the layers is very important for postbuckling behavior of anisotropic plates under shear loading or the combination of compression and shear. This means that the postbuckling behavior of anisotropic plates will depend greatly upon the directions of the shear acting on the plates.

Analysis

Consider a rectangular plate (see Fig. 1) consisting of laminated anisotropic composite materials with a midplane symmetric lay-up. It is assumed that the materials are elastic and the thickness h of the plate is very small compared with the length a and width b. The midplane of the plate before buckling contains the reference coordinate system Oxy with the origin at one of the corners.

The governing equations for postbuckling analysis have been given in Refs. 7 and 8, or elsewhere. In the present case they may be written in the following form

$$\int_0^a\int_0^b \left\{A_{22}^*\frac{\partial^4\phi}{\partial x^4} - 2A_{26}^*\frac{\partial^4\phi}{\partial x^3\partial y} + (2A_{12}^* + A_{66}^*)\frac{\partial^4\phi}{\partial x^2\partial y^2} - 2A_{16}^*\frac{\partial^4\phi}{\partial x\partial y^3} + A_{11}^*\frac{\partial^4\phi}{\partial y^4} + \frac{1}{2}L^*(w_0,w_0)\right\}\delta\phi\,dx\,dy = 0 \quad (1)$$

$$\int_0^a\int_0^b \left\{D_{11}^*\frac{\partial^4 w_0}{\partial x^4} + 4D_{16}^*\frac{\partial^4 w_0}{\partial x^3\partial y} + 2(D_{12}^* + 2D_{66}^*)\frac{\partial^4 w_0}{\partial x^2\partial y^2} + 4D_{26}^*\frac{\partial^4 w_0}{\partial x\partial y^3} + D_{22}^*\frac{\partial^4 w_0}{\partial y^4} - L^*(w_0,\phi)\right\}\delta w_0\,dx\,dy$$
$$+\int_0^b\left[\left(D_{11}^*\frac{\partial^2 w_0}{\partial x^2} + 2D_{16}^*\frac{\partial^2 w_0}{\partial x\partial y} + D_{12}^*\frac{\partial^2 w_0}{\partial y^2}\right)\times\delta\left(\frac{\partial w_0}{\partial x}\right)\right]\Big|_{x=0}^{x=a}dy + \int_0^a\left[\left(D_{21}^*\frac{\partial^2 w_0}{\partial x^2} + 2D_{26}^*\frac{\partial^2 w_0}{\partial x\partial y} + D_{22}^*\frac{\partial^2 w_0}{\partial y^2}\right)\cdot\delta\left(\frac{\partial w_0}{\partial y}\right)\right]\Big|_{y=0}^{y=b}dx = 0 \quad (2)$$

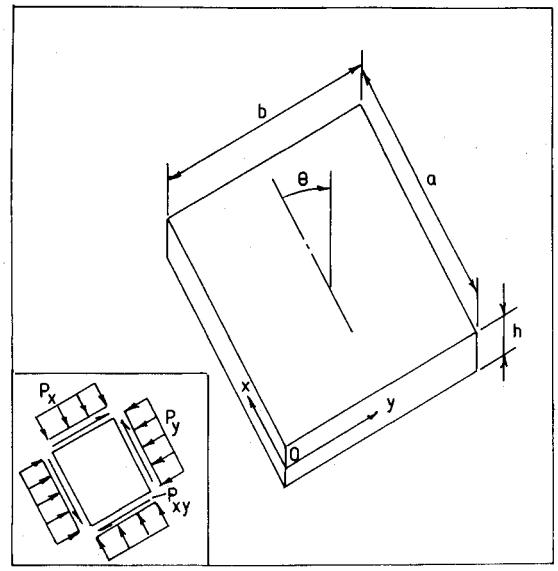

Fig. 1 Definition of positive loading, positive fiber direction and geometry.

Received Aug. 2, 1982; revision submitted April 8, 1983.

*Structural Analyst Engineer, Shenyang Aircraft Company, China. Academic Visitor, Aeronautics Department, Oct. 1980-Oct. 1982.

†Senior Lecturer, Aeronautics Department.

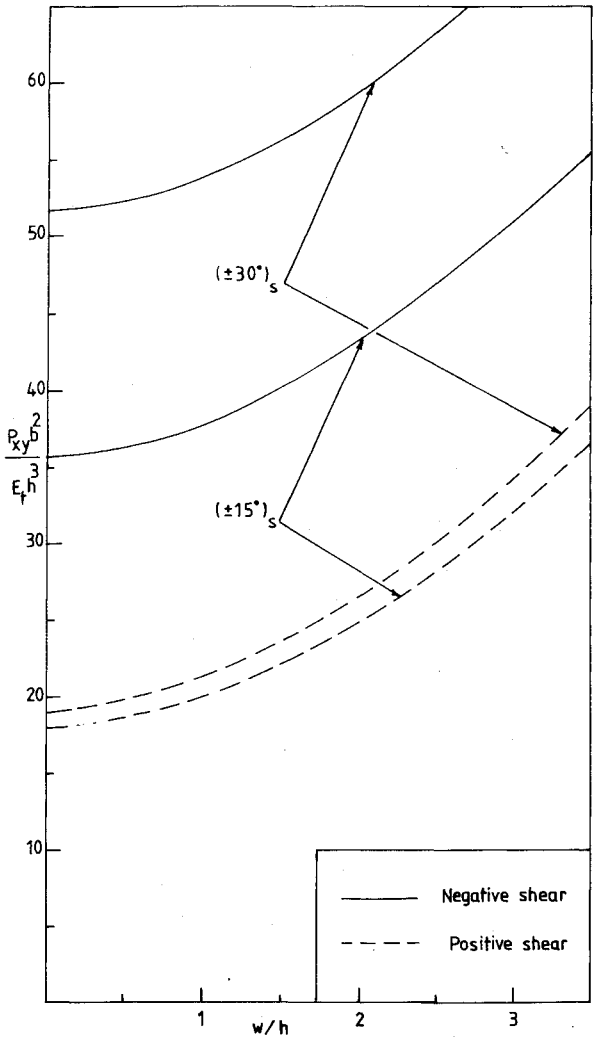

Fig. 2 Variation of nondimensional central deflection with nondimensional load for square boron/epoxy plates with different fiber angles, loaded in pure shear.

where ϕ is the Airy stress function; w_0 the lateral deflection of the plate; A_{ij}^*, D_{ij}^* the reduced stiffness coefficients of the plates, defined as in Ref. 9; and L^* is an operator defined as

$$L^*(A,B)=\frac{\partial^2 A}{\partial x^2}\frac{\partial^2 B}{\partial y^2}+\frac{\partial^2 A}{\partial y^2}\frac{\partial^2 B}{\partial x^2}-2\frac{\partial^2 A}{\partial x\partial y}\frac{\partial^2 B}{\partial x\partial y}$$

Two boundary integrals included in the Eq. (2) represent the effects of edge moments. With these terms the boundary conditions of the edge moments may be satisfied in the mean when the deflection functions cannot satisfy them directly for anisotropic plates.

Introducing the following, and other, nondimesional parameters:

$$w=\frac{w_0}{h},\quad F=\frac{\phi}{A_{22}h^2},\quad \xi=\frac{x}{a},\quad \eta=\frac{y}{b},\quad \beta=\frac{a}{b} \tag{3}$$

The governing system Eqs. (1) and (2) may be written in the nondimensional form

$$\int_0^1\int_0^1\left\{\frac{\partial^4 F}{\partial\xi^4}+a_1\frac{\partial^4 F}{\partial\xi^3\partial\eta}+a_2\frac{\partial^4 F}{\partial\xi^2\partial\eta^2}+a_3\frac{\partial^4 F}{\partial\xi\partial\eta^3}+a_4\frac{\partial^4 F}{\partial\eta^4}\right.$$
$$\left.+a_5\left[\left(\frac{\partial^2 w}{\partial\xi\partial\eta}\right)^2-\frac{\partial^2 w}{\partial\xi^2}\frac{\partial^2 w}{\partial\eta^2}\right]\right\}\delta F\,\mathrm{d}\xi\,\mathrm{d}\eta=0$$

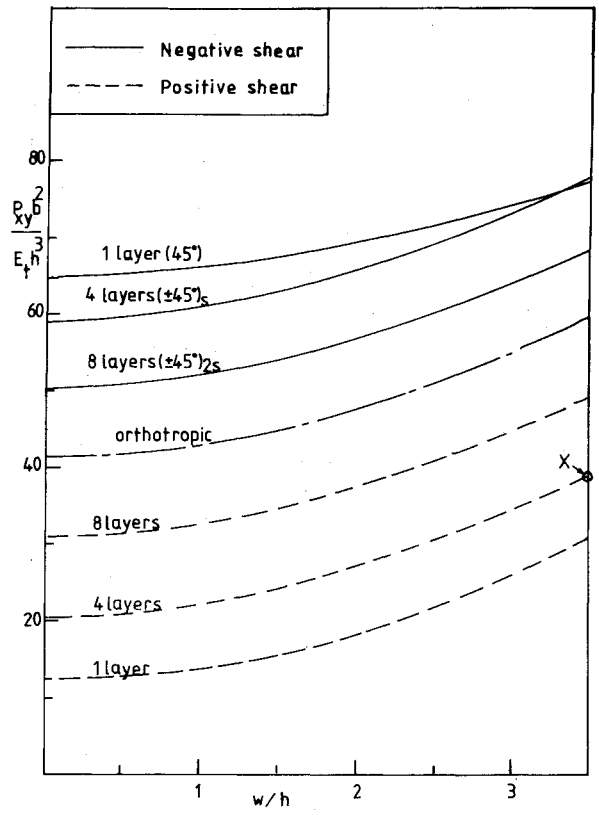

Fig. 3 Variation of nondimensional central deflection with nondimensional load for square boron/epoxy plates with alternate 45 deg layers, loaded in pure shear.

$$\int_0^1\int_0^1\left\{\frac{\partial^4 w}{\partial\xi^4}+b_1\frac{\partial^4 w}{\partial\xi^3\partial\eta}+b_2\frac{\partial^4 w}{\partial\xi^2\partial\eta^2}+b_3\frac{\partial^4 w}{\partial\xi\partial\eta^3}+b_4\frac{\partial^4 w}{\partial\eta^4}\right.$$
$$\left.+b_5\left[\frac{\partial^2 w}{\partial\xi^2}\frac{\partial^2 F}{\partial\eta^2}+\frac{\partial^2 w}{\partial\eta^2}\frac{\partial^2 F}{\partial\xi^2}-2\frac{\partial^2 w}{\partial\xi\partial\eta}\frac{\partial^2 F}{\partial\xi\partial\eta}\right]\right\}\delta w\,\mathrm{d}\xi\,\mathrm{d}\eta$$
$$+\int_0^1\left\{\left(\frac{\partial^2 w}{\partial\xi^2}+b_6\frac{\partial^2 w}{\partial\xi\partial\eta}+b_7\frac{\partial^2 w}{\partial\eta^2}\right)\cdot\delta\left(\frac{\partial w}{\partial\xi}\right)\right\}\Big|_{\xi=0}^{\xi=1}\mathrm{d}\eta$$
$$+\int_0^1\left\{\left(b_8\frac{\partial^2 w}{\partial\xi^2}+b_9\frac{\partial^2 w}{\partial\xi\partial\eta}+b_4\frac{\partial^2 w}{\partial\eta^2}\right)\cdot\delta\left(\frac{\partial w}{\partial\eta}\right)\right\}\Big|_{\eta=0}^{\eta=1}\mathrm{d}\xi=0 \tag{4}$$

If the membrane forces and moments are nondimensionalized as

$$\begin{bmatrix}N_\xi\\N_\eta\\N_{\xi\eta}\end{bmatrix}=\frac{b^2}{A_{22}h^2}\begin{bmatrix}N_x\\N_y\\N_{xy}\end{bmatrix}\text{ and }\begin{bmatrix}M_\xi\\M_\eta\\M_{\xi\eta}\end{bmatrix}=\frac{b^2}{A_{22}h^3}\begin{bmatrix}M_x\\M_y\\M_{xy}\end{bmatrix} \tag{5}$$

Then the boundary conditions for simply-supported edges are

$$w=0,\ M_\xi=0,\ \frac{\partial^2 F}{\partial\eta^2}=-N_1,\ \frac{\partial^2 F}{\partial\xi\partial\eta}=-\beta S \text{ at } \xi=0,1$$

$$w=0,\ M_\eta=0,\ \frac{\partial^2 F}{\partial\xi^2}=-N_2\beta^2,\ \frac{\partial^2 F}{\partial\xi\partial\eta}=-\beta S \text{ at } \eta=0,1 \tag{6}$$

where

$$N_1 = P_x b^2/A_{22}h^2, \quad N_2 = P_y b^2/A_{22}h^2, \quad S = P_{xy} b^2/A_{22}h^2 \tag{7}$$

P_x, P_y are boundary compressive loads in the x or y direction and P_{xy} is the boundary shear load.

The solutions to the governing system Eqs. (4) are assumed to have the following form

$$F = -N_1\frac{\eta^2}{2} - N_2\beta^2\frac{\xi^2}{2} - \beta S\xi\eta + \sum_m \sum_n F_{mn}X_{mn}(\xi)\,Y_{mn}(\eta)$$

$$w = \sum_p \sum_q w_{pq}\sin p\pi\xi \sin q\pi\eta \tag{8}$$

where X_i, Y_i are characteristic beam functions defined as

$$X_i(\xi) = \cosh\alpha_i\xi - \cos\alpha_i\xi - \gamma_i(\sinh\alpha_i\xi - \sin\alpha_i\xi)$$

$$Y_i(\eta) = \cosh\alpha_i\eta - \cos\alpha_i\eta - \gamma_i(\sinh\alpha_i\eta - \sin\alpha_i\eta) \tag{9}$$

Table 1 Values of constants

i	α_i	γ_i
1	4.7300407448627	0.98250221457624
2	7.8532046240958	1.00077731190727
3	10.995607838002	0.99996645012541
4	14.137165491257	1.00000144989766
5	17.278759657400	0.99999993734438
6	20.420352245626	1.00000000270759
7	23.561944902040	0.99999999988299
8	26.7035375555082	1.00000000000506
9	29.8451302091033	0.99999999999978

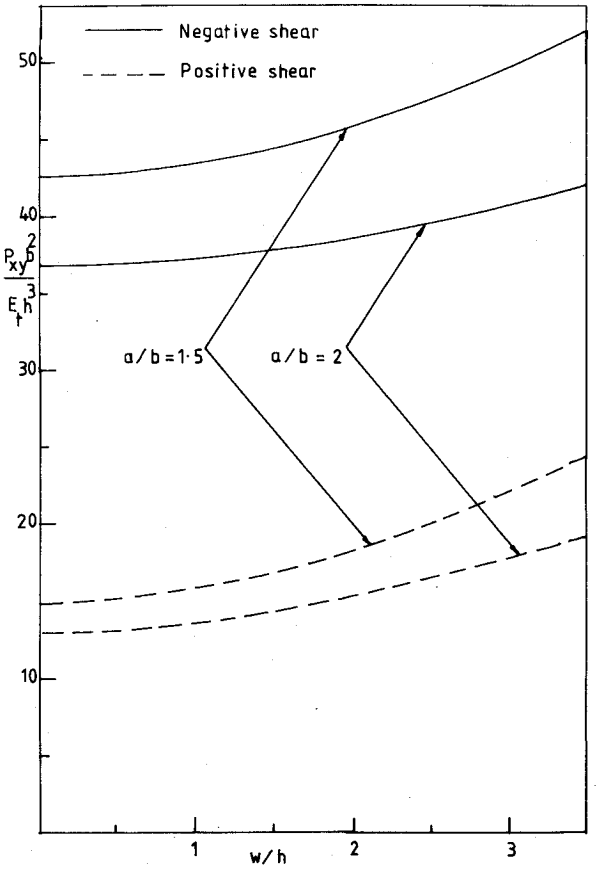

Fig. 4 Variation of nondimensional central deflection with nondimensional load for boron/epoxy plates with $(\pm 45\ \text{deg})_s$ lay-up and different aspect ratios, loaded in pure shear.

in which α_i and γ_i are constants. The values of these constants, with high precision, are suggested in Ref. 5 and listed in Table 1.

With these constants, functions X_i have the following properties

$$X_i(0) = X_i(1) = \frac{dX_i(\xi)}{d\xi}\bigg|_{\xi=0} = \frac{dX_i(\xi)}{d\xi}\bigg|_{\xi=1} = 0 \tag{10}$$

$$\int_0^1 X_i(\xi)X_j(\xi)d\xi = 0, \quad i \neq j$$

$$= 1, \quad i = j \tag{11}$$

and

$$\frac{d^4X_i(\xi)}{d\xi^4} = \alpha_i^4 X_i(\xi) \tag{12}$$

Equations (10-12) also hold for functions Y_i with η replacing ξ.

It may be seen that the assumed solutions of Eq. (8) satisfy the kinematic and in-plane boundary conditions of Eq. (6), but not the zero-moment conditions on the edges due to the coupling terms involving D_{16}^* and D_{26}^*. As mentioned before, however, the effects of the edge moments are taken into account in Eq. (2). Hence, it is necessary only to set the solutions of Eq. (8) into the system Eq. (4). The resultant equations are shown next.

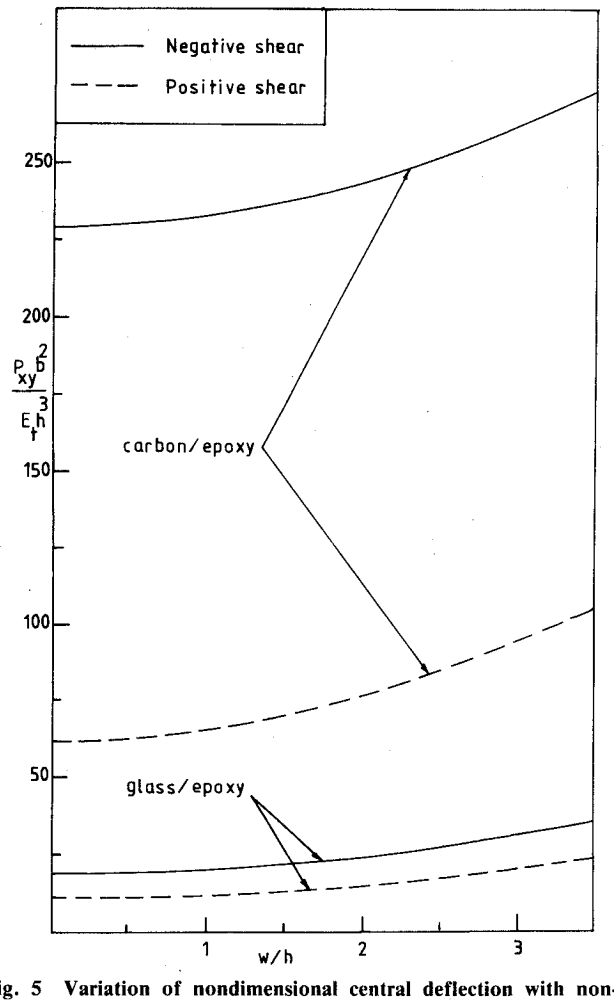

Fig. 5 Variation of nondimensional central deflection with nondimensional load for square plates with $(\pm 45\ \text{deg})_s$ lay-up, made of carbon/epoxy or glass/epoxy composite materials, loaded in pure shear.

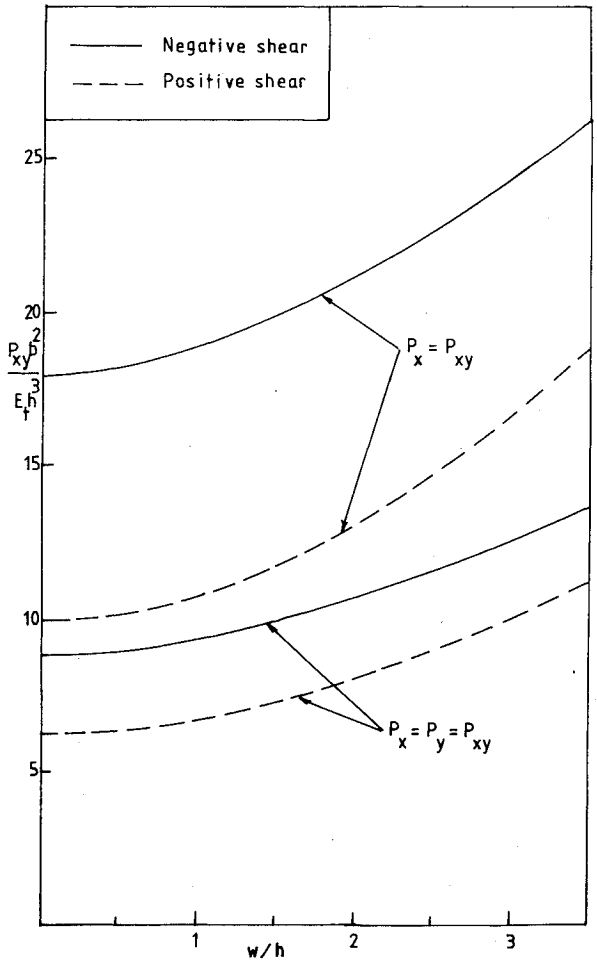

Fig. 6 Variation of nondimensional central deflection with nondimensional load for square boron/epoxy plates with $(\pm 45 \text{ deg})_s$ lay-up under combined shear and compressive loading.

$$\sum_m \sum_n F_{mn} A^{ij}_{mn} = \sum_k \sum_l \sum_r \sum_s w_{kl} w_{rs} B^{ij}_{klrs}$$

$$\sum_p \sum_q w_{pq} C^{ij}_{pq} = \sum_k \sum_l \sum_r \sum_s w_{kl} F_{rs} D^{ij}_{klrs}$$

$$+K \sum_p \sum_q w_{pq} T^{ij}_{pq} \qquad (i,j=1,2,3,\ldots) \qquad (13)$$

where $K=Pb^2/E_t h^3$ and P is related to the applied loads by λ_x, λ_y and λ_s which are defined as

$$P_x=\lambda_x P, \quad P_y=\lambda_y P, \quad P_{xy}=\lambda_s P$$

By properly choosing the ratio between λ_x, λ_y, and λ_s, one may have any required combination of boundary loading.

The terms A^{ij}_{mn}, B^{ij}_{klrs}, C^{ij}_{pq}, D^{ij}_{klrs}, and T^{ij}_{pq} depend on various material and geometric parameters and also terms which are integrals of the functions X_i and Y_i, their derivatives and the constant α_i.

Computation and Results

In order to obtain the postbuckling path, an iterative scheme is used for the governing system. The starting point of the iteration is based on the characteristic solution of bifurcation, corresponding to the lowest critical load. By dropping the nonlinear terms from the second equation of system (13) the characteristic equations may be obtained in the matrix form

$$[C]\{w\}=K[T]\{w\}$$

The QZ algorithm is used here to obtain the lowest eigenvalue $K_{\min}$ and the corresponding eigenvector $\{w^{(0)}\}$ which represents the buckling mode for initial buckling of the plate.

The method for solving the postbuckling path consists of prescribing one of the components of $\{w\}$ and letting it increase step-by-step. Correspondingly, the other components of $\{w\}$ and the load parameter K, from the governing system of Eq. (13) are found by the use of a hybrid iterative scheme (a modified Newton's method). Thus, a series of points on the postbuckling path can be obtained. At the beginning of the process, the first estimate used for the iteration at each new point is the solution belonging to the last point except for the prescribed component of $\{w\}$. After three points are obtained, an extrapolation scheme is introduced to make a better estimation for every next point. In the process the function F is solved from the first expression of Eq. (13) and set in the second one of that set.

The component having the largest absolute value in the characteristic solutions $\{w^{(0)}\}$ is the one prescribed. The step length varies from 0.1 to 0.6 for different plates. The convergence criterion used for iteration is that the sum of the squares of the residuals of the governing equations is less than 0.01%.

A series of computations is carried out for various plates. In the current investigation the first 25 terms only for the solution of Eq. (8) are used. Only plates with symmetric lay-ups are considered in the present paper and such plates can be expected to demonstrate the "pure" bifurcation behavior described earlier. Plates with other lay-ups, however, may bend immediately when load is applied. This phenomenon will be discussed in a separate paper.

Table 2 Material properties for computations

	E_l/E_t	G_{lt}/E_t	ν_{lt}
Boron/epoxy	10	0.25	0.3
Carbon/epoxy	40	0.5	0.25
Glass/epoxy	3	0.5	0.25

The material properties of boron/epoxy, carbon/epoxy, and glass/epoxy used for the computations are shown in Table 2. The computation results are summarized in the figures and all refer to plates with a width to thickness ratio $b/h=100$.

Results for square boron/epoxy plates under pure shear are shown in Figs. 2 and 3. These figures show how the deflection at the center of the plates varies with increasing shear loading after buckling. It can be seen that there are two postbuckling paths for each plate according to the direction of the applied shear, unless the plate is orthotropic. In Fig. 2 it is shown that for a four-layer plate even fiber angles as small as 15 deg in the alternate layers may cause a large difference in the postbuckling behavior of the plate. Figure 3 shows the influence of the number of alternate 45 deg layers. It is clear that the less the number of layers, the larger are the differences that exist between the postbuckling paths corresponding to alternate directions of applied shear. A plate will behave as if orthotropic only when the number of layers in it becomes very large.

As may be expected different post-buckling paths are also obtained for rectangular plates. This effect is demonstrated in Fig. 4, again for boron/epoxy material in pure shear, but here with $(\pm 45 \text{ deg})_s$ lay-up.

Figure 5 refers to pure shear loading of square plates having a $(\pm 45 \text{ deg})_s$ lay-up of carbon/epoxy or glass/epoxy materials. The curves of central deflection vs loading show that for the carbon/epoxy plate, which has the higher ratio of E_l/E_t for the composite, the difference between the post-

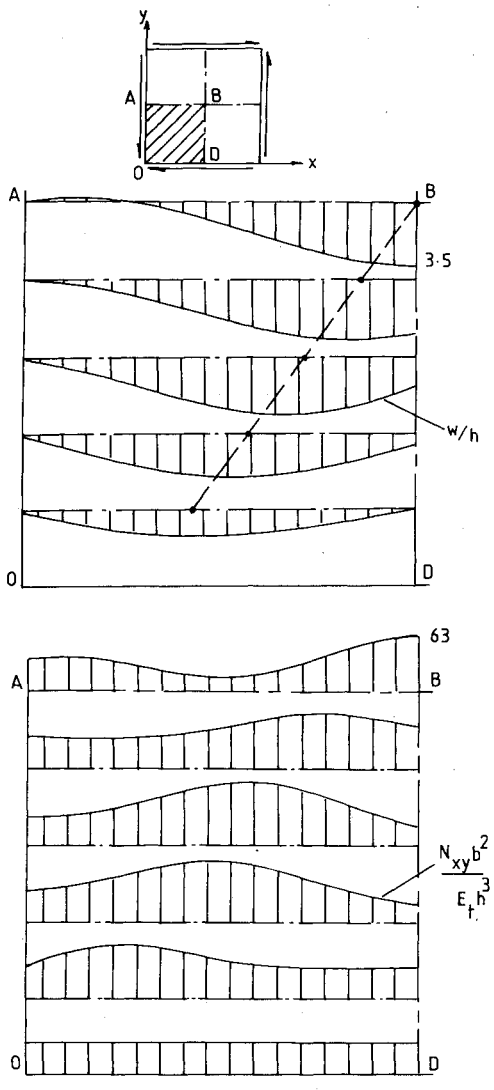

Fig. 7 Distribution of lateral deflection and internal shear force over one quarter of a square boron/epoxy plate with $(\pm 45 \text{ deg})_s$ lay-up, loaded in pure shear.

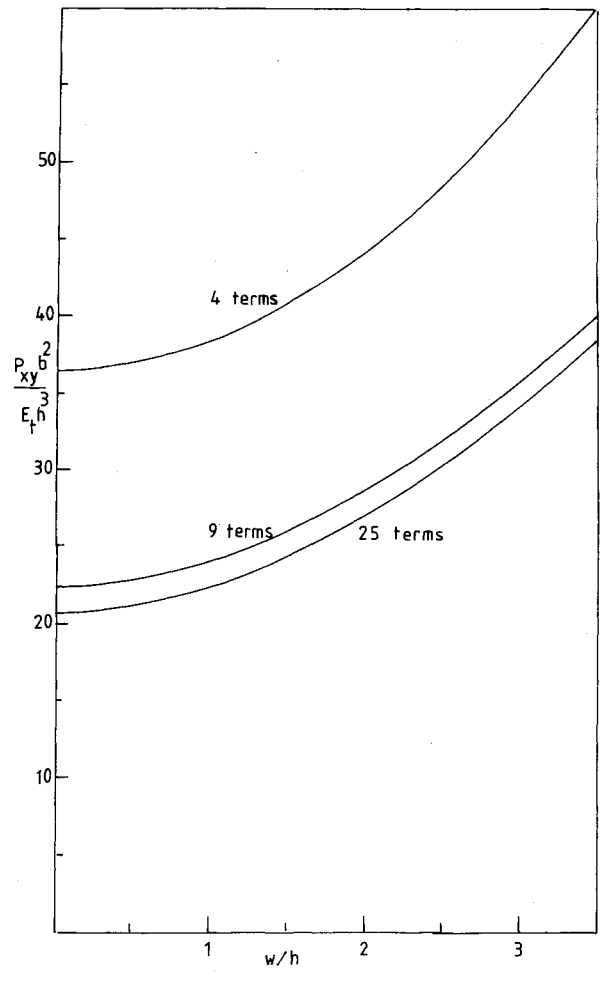

Fig. 8 Comparison of the results obtained for different solution approximations.

buckling paths for alternate shear directions is larger than for the glass/epoxy plate. Corresponding curves for boron/epoxy may be found in Fig. 3.

Similar results are obtained for combined loading, i.e., shear applied simultaneously with either unidirectional or bidirectional compressive loads. The results shown in Fig. 6 again apply to a square boron/epoxy plate with $(\pm 45 \text{ deg})_s$ lay-up. Comparing with the curves for pure shear given in Fig. 3, it is seen that combined loading reduces the buckling strength and reduces the distance between the paths corresponding to alternate shear directions. As would be expected, these changes are more marked for bidirectional compression.

The variation across the plate of the membrane shear stress resultant (N_{xy}) and the lateral deflection are also of interest. The distribution of these quantities over one quarter of a square plate are shown in Fig. 7, also for a $(\pm 45 \text{ deg})_s$ lay-up of boron/epoxy. The load corresponds to point X on Fig. 3. It is found that the points at which the largest deflection occurs on the selected sections may be connected approximately by a straight line. Although close to, this line is not coincident with the plate diagonal because of the anisotropy of the plate. In the figure it is also seen that the distribuiton of N_{xy} is nonuniform at all the sections selected, apart from the edge.

In order to determine the accuracy of the 25-term approximation used for the solutions, the results for a square boron/epoxy plate with $(\pm 45 \text{ deg})_s$ lay-up, under positive shear, is shown in Fig. 8 for different numbers of terms. It is seen that the 25-term solution is sufficient for most engineering purposes.

Conclusions

The following conclusions may be drawn from the current investigation.

1) For anisotropic plates of symmetrically laminated composite materials loaded in shear, there are two post-buckled paths corresponding to alternate shear directions. The difference between these two paths is affected greatly by the lay-up of laminae, the properties of the composite, and the aspect ratios of the plates. A high ratio of E_l/E_t and small number of layers will result in a big difference between the two paths.

2) The postbuckling behavior of anisotropic plates under combined compression and shear loading is also affected significantly by the direction of the shear, whether unidirectional or bidirectional compression acts on the plates. However, the difference is less than when the plate is subjected to pure shear.

3) The higher performance of a composite plate occurs when the direction of the applied shear forces produces a tension resultant in the diagonal of the plate having the lower bending stiffness. For a prescribed direction of shear, however, the peformance of the plate depends on the direction of the fiber angles of the layers, especially of the outer layers.

References

[1]Kaminski, B. E. and Ashton, J. E., "Diagonal Tension Behavior of Boron/Epoxy Shear Panels," *Journal of Composite Materials*, Vol. 5, Oct. 1971, pp. 553-558.

[2]Kobayashi, S., Sumihara, K. and Koyama, K., "Shear Buckling Strength of Graphite-Epoxy Laminated Panels," *Composite Materials, Proceedings of Japan-U.S. Conference*, Tokyo, 1981.

[3]Sumihara, K., Kobayashi, S., and Koyama, K., "Shear Buckling Strength of CFRP Laminated Panels (1st Report)," *Journal of the Japan Society for Aeronautical and Space Sciences*, Vol. 29, June 1981, pp. 321-332.

[4]Ashton, J. E. and Whitney, J. M., *Theory of Laminated Plates*, Technomic Publishing Co. Inc., Lancaster, Pa., 1970.

[5]Zhang, Y. and Matthews, F. L., "Initial Buckling of Curved Panels of Generally Layered Composite Materials," *International Journal of Composite Structures*, Vol. 1, July 1983, pp. 3-30.

[6]Zhang, Y. and Matthews, F. L., "The Effect of the Directions of Combined Shear on the Compressive Buckling Load of Generally Laminated Plates," *Proceedings of the Conference ICCM IV*, Japan Society for Composite Materials, Tokyo, Oct. 1982.

[7]Chia, C. Y., *Nonlinear Analysis of Plates*, McGraw-Hill Intl., New York, 1980.

[8]Zhang, Y. and Matthews, F. L., "The Postbuckling Behavior of Curved Panels of Generally Layered Composite Materials," *International Journal of Composite Structures*, Vol. 1, Oct. 1983, pp. 115-136.

[9]Jones, R. M., *Mechanics of Composite Materials*, Scripta Book Co., Washington, D.C., 1975.